A Journal of the Gesellschaft Deutscher Chemiker

Angewandte International Edition GDCh Chemie

www.angewandte.org

Accepted Article

Title: Phenotyping reveals the targets of a pseudo-natural product autophagy inhibitor

Authors: Herbert Waldmann, Daniel J. Foley, Sarah Zinken, Dale Corkery, Luca Laraia, Axel Pahl, and Yaowen Wu

To be cited as: *Angew. Chem. Int. Ed.* 10.1002/anie.202000364
Angew. Chem. 10.1002/ange.202000364

Link to VoR: http://dx.doi.org/10.1002/anie.202000364
http://dx.doi.org/10.1002/ange.202000364

WILEY-VCH

10.1002/anie.202000364

Phenotyping reveals the targets of a pseudo-natural product autophagy inhibitor

Daniel J. Foley,[a,b] Sarah Zinken,[a,c] Dale Corkery,[d] Luca Laraia,[a,e] Axel Pahl,[a,f] Yao-Wen Wu,[d] Herbert Waldmann*[a,c]

Dedicated to Prof. Dr. Rolf Huisgen on the occasion of his 100th birthday.

[a]Max Planck Institute of Molecular Physiology, Dortmund, Germany.

[b]Current address: School of Physical and Chemical Sciences, University of Canterbury, Christchurch, New Zealand.

[c]Faculty of Chemistry and Chemical Biology, Technical University Dortmund, Dortmund, Germany.

[d]Department of Chemistry, Umeå Centre for Microbial Research, Umeå University, Umeå, Sweden.

[e]Current address: Department of Chemistry, Technical University of Denmark, Copenhagen, Denmark.

[f]Compound Management and Screening Centre, Dortmund, Germany.

*Corresponding email: herbert.waldmann@mpi-dortmund.mpg.de

Keywords

Pseudo-natural products, autophagy, phenotyping, alkaloids, inhibitors, chemical biology.

Abstract

Principles for the design and synthesis of novel bioactive compounds can efficiently draw from insights gained into natural product (NP) structure and bioactivity, including complexity-to-diversity approaches and biology-oriented synthesis. Pseudo-natural product design goes beyond these principles, and combines natural product fragments to provide unprecedented NP-inspired compounds not accessible by biosynthesis, yet endowed with biological relevance. Since the bioactivity of pseudo-NPs may be unprecedented or unexpected, they are best evaluated in target agnostic cell-based assays monitoring entire cellular programs or complex phenotypes. We have merged the Cinchona alkaloid scaffold with the indole ring-system to synthesise 'indocinchona alkaloids' *via* an efficient Pd-catalysed annulation. Exploration of indocinchona alkaloid bioactivity in

phenotypic assays revealed a novel class of azaindole-containing autophagy inhibitors, the 'azaquindoles'. Subsequent characterisation of the most potent compound, azaquindole-1, in the morphological "cell painting" assay, guided target identification efforts which revealed that, in contrast to the parent Cinchona alkaloids, azaquindoles selectively inhibit starvation- and rapamycin-induced autophagy by targeting the lipid kinase VPS34.

Natural products (NPs)[1] occupy a definable area of chemical space,[2] and are notable for their diverse frameworks and shapes, stereochemical complexity, heteroatom content, high fraction of sp^3-hybridised atoms and diverse bioactivity. Significant focus has been placed on the design and preparation of biologically relevant small molecules endowed with NP-like features.[3,4] Recently developed design strategies include complexity-to-diversity (CtD) approaches, in which alternative NPs[4] or complex synthetic intermediates[5] are modified or distorted; and biology-oriented synthesis (BIOS),[3] in which NP structure is simplified, to arrive at synthetically tractable NP-derived scaffolds. We very recently introduced 'pseudo-natural products' as novel compounds with NP-like structures and properties.[6–11] Pseudo-NPs are obtained through the unprecedented combination of NP-derived fragments and occupy areas of biologically relevant chemical space inaccessible to nature through biosynthesis.[12] There is an urgent requirement for unbiased biological profiling of these new compounds, since their possible biological activities are unknown.

For the design of a new pseudo-NP class we were drawn towards a biologically-unprecedented fusion of the biosynthetically-related[13,14] Cinchona **1-4** and indole alkaloids, which promised to yield a new pseudo-NP class with unexpected bioactivity. For efficient synthesis of an 'indocinchona alkaloid' library (Figure 1a-b) we envisioned to combine the indole ring system *via* an edge-on-edge, 2,3-fusion as found in a variety of alkaloids (e.g. catharanthine, yohimbine),[13] directly onto the caged quinuclidine ring-system of the Cinchona alkaloids, which is biologically-unprecedented. Here, we describe the expedient use of a Pd-catalysed annulation to prepare the envisioned indocinchona alkaloid library (Figure 1b-c).[15] Biological investigation of the collection, including phenotypic characterisation of bioactivity in an unbiased, multiparametric "cell painting" assay revealed a new inhibitor of both starvation- and rapamycin-induced autophagy, which targets the lipid kinase VPS34.

For 2,3-fusion of the indole ring system to the Cinchona alkaloids, a unifying, operationally straightforward, and preferably one-pot connective reaction was required. It was envisioned that the known[16] Cinchona alkaloid-derived ketones **5-6** would provide suitable coupling partners to undergo regioselective Pd-catalysed annulations with 2-iodoanilines,[15] to furnish the target pseudo-NPs in a single step (Figure 1c).

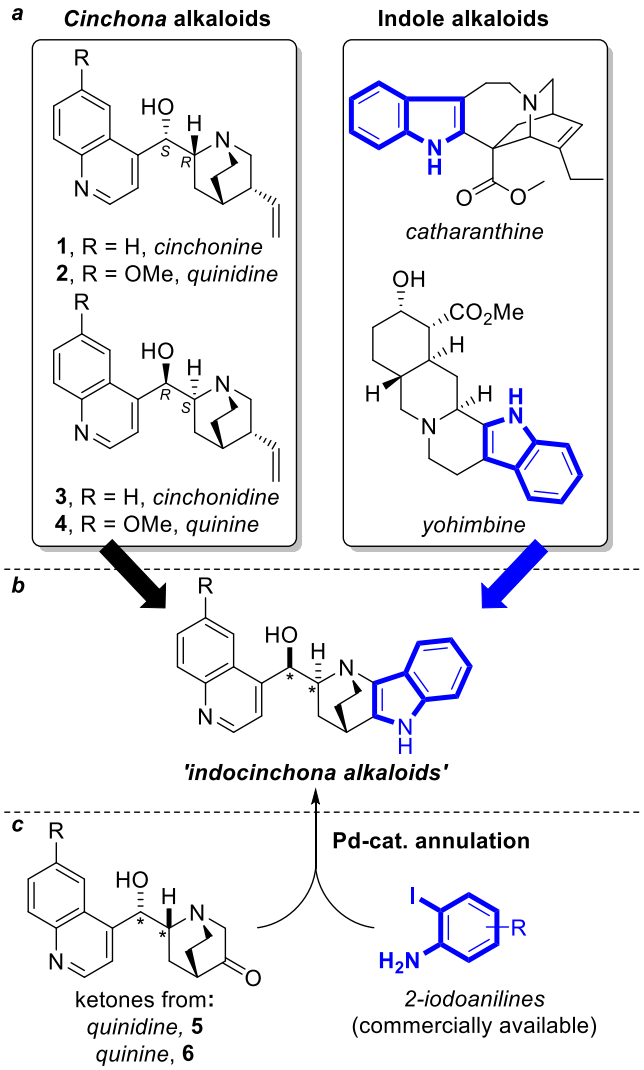

Figure 1. Proposed design strategy to derive novel indole alkaloids from the Cinchona alkaloids: (a) The Cinchona alkaloids and representative 2,3-fused indole alkaloids; (b) The targeted unnatural indole alkaloids derived from Cinchona alkaloids; (c) Proposed synthetic route to the pseudo-NPs by harnessing a Pd-catalysed annulation between the quinidine/quinine-derived ketones **5-6** and 2-iodoanilines. *Stereochemistry relative to compounds **1-2** as appropriate.

For the synthesis of ketones **5** and **6** the quinine/quinidine terminal alkenes were isomerised[17] to internal alkenes **7-8** which were oxidatively cleaved under modified Lemieux–Johnson conditions[16] to give the ketones **5-6** in a telescoped two-step procedure in 38% and 50% yields respectively (Figure 2a-b).

For the envisioned Pd-catalysed Heck-type annulation we employed the ligand-free variant developed by Chen *et al.*[15] and, pleasingly, exposure of the ketones **5-6** to 2-iodoanilines in the presence of catalytic $Pd(OAc)_2$ and DABCO provided the targeted pseudo-NP compounds in viable yields and in multimilligram amounts. 2-Iodoanilines bearing a range of polar functionalities, including nitro and carboxylic acid functional groups at the 3-6 positions were tolerated and the reaction protocol was successfully extended to the preparation of 6- and 7-azaindoles (**9**-**10v** and **9**-**10w**). Overall, the indole synthesis proved to be very robust and yielded a collection of 61 indocinchona alkaloids in total (Figure 2a-b and SI Section 3).

A substructure search in the Dictionary of Natural Products (DNP) revealed that both the indocinchona alkaloid scaffold, and the fused quinuclidine-indole ring-system, were not found in NPs (see Figure S1 for substructure searches). Comparison of the NP-likeness[18] of the collection with the guiding Cinchona alkaloid NPs **1**-**4**, NPs from ChEMBL,[19] and drugs from DrugBank (Figure 2c)[20] revealed that the indocinchona alkaloids display a narrow NP-score distribution (μ[NP-likeness score] = –0.04), and contain connectivity that is more 'synthetic compound-like' than both the guiding Cinchona alkaloids (+0.83), and NPs in general (μ = +1.95). The average scores for the indocinchona alkaloids are close to the scores for compounds in DrugBank (μ = –0.01, and +0.02, respectively).

Shape analysis of the compound collection by generating the two normalised principal moments of inertia values (Figure 2d)[21] indicated that the collection has a wide distribution of molecular shapes and a high three-dimensional character. The indocinchona alkaloids also exhibit a high fraction of sp^3-hybridised carbons (μ[Fsp^3] = 0.30), a valuable feature for the successful progression of drug candidates.[22] Overall the library has favourable properties for molecular discovery,[23] with 96% of the compounds falling within Lipinksi "Rule-of-5" space (Figure S2).[24]

10.1002/anie.202000364

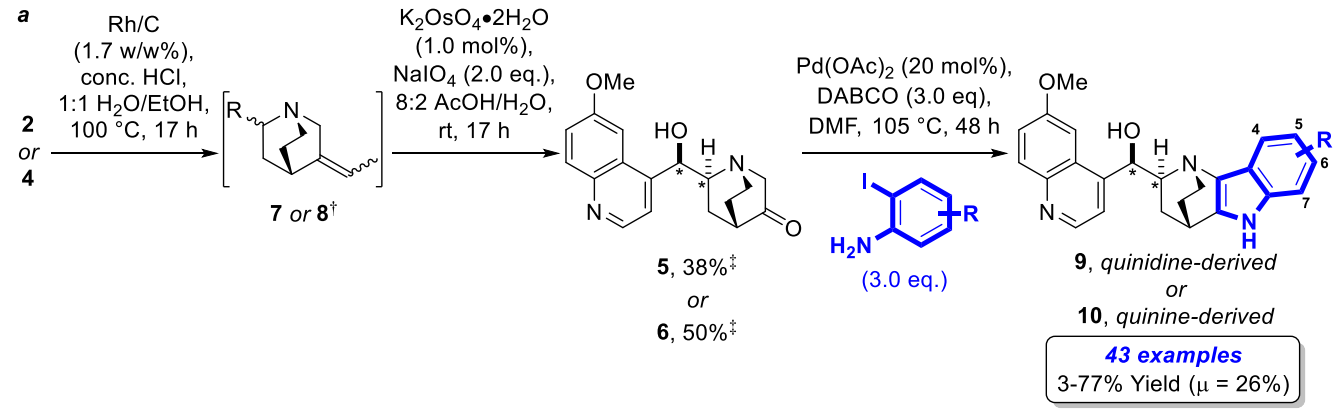

b

4, 5, 6, 7 = R = H:
9a (49%); **10a** (17%)

4 = R; 5-7 = H. R =
Me: **9b** (49%); **10b** (46%)
CO_2Me: **9c** (18%)[a]; **10c** (12%)[a]
Cl: **9d** (77%)[b]; **10d** (10%)[b]

5 = R; 4, 6-7 = H. R =
Me: **9e** (45%); **10e** (17%)
CO_2H: **9f** (14%)[a,d]; **10f** (9%)[b,d]
CO_2Me: **9g** (3%)[a,d]
CF_3: **9h** (25%); **10h** (23%)[a]
NO_2: **9i** (12%)[a,d]; **10i** (3%)[a,d]
OMe: **9j** (23%)[a,c]; **10j** (6%)[a]
OCF_3: **10k** (65%)[b]
F: **9l** (19%)[d]; **10l** (47%)
Cl: **9m** (48%); **10m** (59%)[b,d]
Br: **9n** (8%)[d]; **10n** (15%)

6 = R; 4-5, 7 = H. R =
Me: **9o** (12%)[a,d]; **10o** (4%)
CO_2H: **9p** (11%)[b,d]; **10p** (14%)[d]
CO_2Me: **9q** (7%)[a]
CF_3: **9r** (25%); **10r** (70%)[b]
Cl: **9s** (26%); **10s** (20%)
Br: **9t** (9%)[a,d]; **10t** (27%)[a]

7 = R; 4-6 = H. R =
OMe: **9u** (16%)[a,d]; **10u** (33%)[a,d]

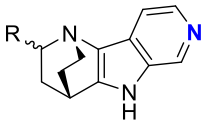

9v (50%)[d];
10v (65%)[b]

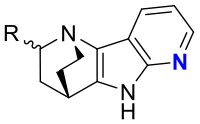

9w (17%)[d];
10w (13%)[a,d]

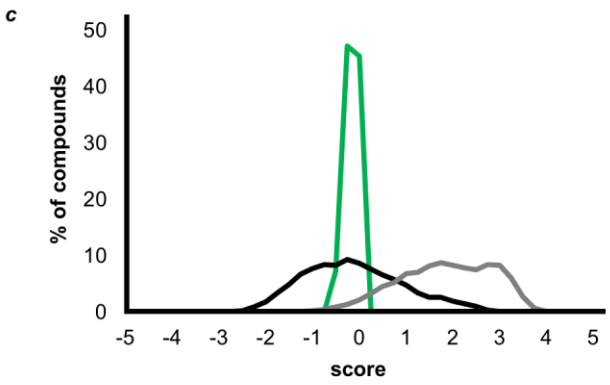

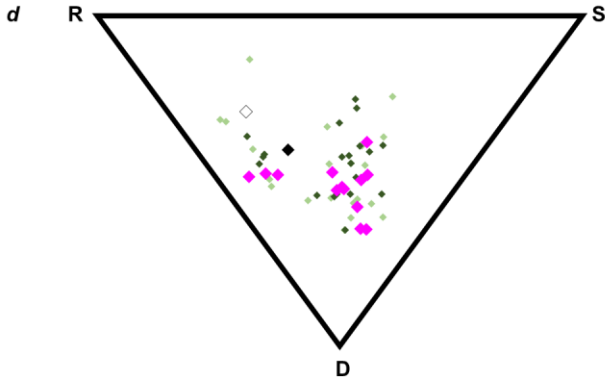

Figure 2. Preparation and chemoinformatic analysis of the novel indole alkaloids **9**-**10**: (a) Synthetic route to prepare compounds **9**-**10**; (b) Library members and yields from the Pd-cat. annulation; (c) NP-likeness scores comparing the indocinchona library (green) with natural products (from ChEMBL, grey) and marketed drugs (DrugBank, black). The data are binned into histograms (0.25 units in width). N.b. the score for quinine/quinidine is +0.83. Scores were calculated using the method developed by Ertl,[18] implemented in RDKit;[25] (d) Shape analysis (PMI) plot of the indocinchona alkaloids versus three idealised molecular shapes (R = rod; D = disk; S = sphere):- quinidine **2** (white); quinine **4** (black); indoquinidines **9a-w** (light green); indoquinines **10a-v** (dark green); 7-azaindoquinines **10w** to **10w-l** (pink). Generated by LLAMA.[21] *Stereochemistry relative to compounds **1**-**2** as appropriate. †In each case a 2:1 mixture of E/Z alkenes was observed. ‡Yields given over 2-steps. [a]30 mol% $Pd(OAc)_2$, 72 h. [b]10 mol% $Pd(OAc)_2$, 24 h. [c]The iodoaniline HCl salt and 6.0 eq. DABCO were used. [d]Isolated as the TFA salt. μ = mean. All yields are unoptimised.

Since phenotypic screening enables identification of bioactivity of new small molecule classes in an unbiased manner,[26–28] we subjected the compound collection to a range of cell-based screens, including a phenotypic assay that monitors autophagic flux (Table 1).[29] Autophagy degrades and recycles superfluous or damaged proteins and organelles *via* autophagosomes. Autophagy plays a crucial role in degenerative diseases and

cancer, and novel small molecule autophagy inhibitors may provide inspiration for new drug discovery programmes.[30,31]

To identify autophagy inhibitors we monitored puncta formation in MCF7 cells stably transfected with an EGFP-tagged LC3 protein (MCF7-EGFP-LC3 cells) upon autophagy induction by amino acid starvation, or treatment with the mTOR inhibitor rapamycin, using high-throughput automated image acquisition and analysis.[32] Use of the autophagosome-autolysosome fusion inhibitor chloroquine (CQ) enhanced the dynamic range of the assay.

Compounds **10**, derived from quinine, inhibited starvation-induced autophagy (Table 1, Entries 1-9), but no inhibitory activity was observed for the quinidine-derived indoles **9a-w** at 10 μM. Compounds **10** substituted at the 5- and 6- positions of the indole ring (Entries 1-7) were relatively weak inhibitors of starvation-induced autophagy ($IC_{50} \approx 4.7–8.1$ μM). Compounds **10** substituted with polar functionalities at the 7-position of the indole ring (Entries 8-9) gave appreciably higher activities. Thus, 7-azaindole-substituted compound **10w** inhibited starvation-induced autophagy with $IC_{50} = 4.33 \pm 1.7$ μM, whilst the 7-methoxy substituted indole **10u** gave the most active initial compound with $IC_{50} = 2.46 \pm 0.6$ μM. Notably, the latter two compounds (Entries 8-9) also inhibited rapamycin-induced autophagy, suggesting that they act downstream or independently of mTOR.

10.1002/anie.202000364

Entry	Compound	R-group and position	starvation-induced IC_{50} /μM	rapamycin-induced IC_{50} /μM
1	**10h**	5-CF_3	7.86 ± 0.8	n/a
2	**10i**	5-NO_2	7.33 ± 1.5	n/a
3	**10k**	5-OCF_3	4.68 ± 1.4	n/a
4	**10m**	5-Cl	5.54 ± 2.5	n/a
5	**10n**	5-Br	6.78 ± 1.1	n/a
6	**10r**	6-CF_3	5.82 ± 3.0	n/a
7	**10s**	6-Cl	8.12 ± 1.5	n/a
8	**10u**	7-OMe	2.46 ± 0.6	2.37 ± 0.7
9	**10w**	7-azaindole	4.33 ± 1.7	4.95 ± 0.7
10	**10w-a**	4-Cl-7-azaindole	0.52 ± 0.20	0.65 ± 0.35
11	**10w-b**	5-Me-7-azaindole	0.31 ± 0.09	0.86 ± 0.26
12	**10w-c**	5-Ar-7-azaindole	9.00 ± 1.1	n/a
13	**10w-d**	5-CF_3-7-azaindole	0.12 ± 0.03	0.77 ± 0.29
14	**10w-e**	5-NO_2-7-azaindole	0.67 ± 0.13	1.26 ± 0.20
15	**10w-f**	5-F-7-azaindole	n/a	n/a
16	**10w-g**	5-Cl-7-azaindole	0.11 ± 0.04	0.85 ± 0.14
17	**10w-h**	5-Br-7-azaindole	0.08 ± 0.03	0.81 ± 0.35
18	**10w-i**	5-I-7-azaindole	0.08 ± 0.02	1.24 ± 0.20
19	**10w-j** (azaquindole-1)	5-Br-6-Me-7-azaindole	0.04 ± 0.02	0.10 ± 0.02
20	**10w-k**	6-Me-7-azaindole	3.12 ± 0.5	5.11 ± 1.4
21	**10w-l**	6-Cl-7-azaindole	3.06 ± 0.9	6.21 ± 2.2
22	**9w**	7-azaindole	n/a	nd
23	**9w-b**	5-Me-7-azaindole	n/a	nd

Table 1. Identification of Cinchona alkaloid-inspired inhibitors of starvation and/or rapamycin-induced autophagy, derived from quinine. All data are shown as mean ± SD of three independent experiments (N = 3; n ≥ 3). All compounds were initially assayed at a concentration of 10 μM. For hits reducing the number of LC3 puncta by more than 50%, IC_{50} values were determined. n/a = inactive (no reduction of LC3 puncta at 10 μM). Ar = 4-Cl-C_6H_4. nd = not determined.

In general, 7-azaindoles were potent, sub-μM inhibitors of autophagy (Table 1, Entries 10-21. See Table S1 for synthetic yields). Introduction of a chlorine at the 4-position of the 7-azaindole (R = Cl, Entry 10) gave an inhibitor of starvation- and rapamycin-induced autophagy with sub-μM activity. Introduction of substituents at the 5-position of the 7-azaindole ring-system (Entries 11-18) revealed that polar (e.g. NO_2; Entry 14) or lipophilic (e.g. Me, CF_3, Cl, Br, I; Entries 11, 13, 16-18) substituents led to nM activities in starvation-induced autophagy, and low- or sub-μM activities in rapamycin-induced autophagy. Markedly, while electronic factors cannot be ruled out, the size of the substituent seems to significantly impact the activity. The small fluoride -substituted 7-azaindole **10w-f** (Entry 15) is inactive, whilst nM inhibition of starvation-induced autophagy is observed for larger halogen substituents (Entries 16-18). Furthermore, the aryl substituted analogue **10w-c**

(Entry 12) leads to diminished inhibitory activity versus the unfunctionalised 7-azaindole (Entry 9). Substitution at the 6-position of the 7-azaindole ring-system does not appear to significantly improve inhibitory activity (Entries 20-21). Surprisingly, however, substitution at both the 5- and 6-positions (with Br and Me, respectively, Entry 19) of the 7-azaindole ring-system gave compound **10w-j**, which had the highest observed inhibitory activity against both starvation- and rapamycin-induced autophagy (0.04 ± 0.02 μM and 0.10 ± 0.02 μM, respectively, Figure 3d-g). We termed the active, quinine-derived 7-azaindole compounds 'azaquindoles'. Compound **10w-j** ('azaquindole-1') was chosen as a potent, representative member for further investigations.

Investigation of **10w-j** analogues, in which various molecular features were either masked or truncated (Figures S3-4) in the autophagy assay determined that the key feature of the compound for inhibition of rapamycin- and –starvation induced autophagy is the fused quinuclidine/azaindole ring system; while substituents at the azaindole 5-position and the presence of the quinoline ring are key drivers of potency. Importantly, the enantiomeric, quinidine-derived, 7-azaindoles (**9w**, **9w-b**, **9w-k**) were inactive in the autophagy assays, as were the parent Cinchona alkaloids (Table S1 and Figure S5). The inhibition of autophagy was not an activity shared by simple indoles, 7-azaindoles, quinuclidines, or quinolines (Figure S5). Indole-containing natural products (82 compounds) within our in-house library were also found to be inactive against autophagy (Table S2). Thus, the azaquindole **10w** bioactivity is not shared by the individual NP fragments.

To gain insight into mode of action and point towards potential targets, pseudo-NPs **10w** were subjected to a non-biased phenotyping assay.[9,33–37] Using image-based analysis, the 'cell painting' morphological profiling assay measures and quantifies a large number of phenotypic changes to cells upon treatment with a compound of interest (COI) which then are condensed in a fingerprint profile (see SI Section 5.3 for details). High similarity to profiles generated for reference compounds that have annotated biological activities (and/or modes of action) may indicate particular molecular targets. Investigation of the sub-μM active 5-substituted members of the **10w** series in the cell painting assay revealed two common reference compounds: the VPS34 inhibitor, SAR405, and the β_2 adrenergic receptor agonist, terbutaline (Figure 3a-c). Investigation of the *in vitro* inhibitory activity of **10w-j** against the β_1 and β_2 adrenergic receptors revealed no agonistic activity

against both receptors, and low antagonistic activity (8.6% and 22% inhibition for β_1 and β_2 respectively). The weak activity suggested that the β_1 and β_2 adrenergic receptors were unlikely to be relevant to the autophagy inhibition activity observed. In addition, **10w-d** showed no inhibitory activity against either receptor. Excitingly, however, VPS34 was inhibited by **10w-j** at 350 nM *in vitro*. Significantly, PI3K kinase PIK3C3/VPS34 plays an important role in autophagosome biogenesis downstream of mTOR.[38]

In order to determine the selectivity of compound **10w-j**, it was screened against the wider kinome (485 kinases), which revealed inhibition of seven additional kinases with IC_{50} values <10 μM (Table S3). Most notably, **10w-j** demonstrated inhibition of a number of PI3Ks (Entries 2-3, 5, 7-8), and of CLK-2 and -4 kinases. In light of the medium nanomolar cellular potency of azaquidole-1 (see Table 1, entry 19) kinase inhibition with sub-μM activity was deemed most relevant. Inhibition of CLK2 and -4 is likely not relevant since the CLK2/4 kinase inhibitor ML167, and the CLK2/3/4 inhibitor TG003, were inactive in the autophagy assay at 10 μM (Table S4). We have previously shown that inhibition of PIK3C2G and PI4KB using several highly potent and selective inhibitors does not result in autophagy inhibition.[39] Additionally, respective investigation of selective SPHK2 and PIK3CD inhibitors in the autophagy assay devalidated likely inhibitory roles for these kinases (Table S4). Across the azaquindole class, inhibition of VPS34 activity correlated strongly with autophagy inhibitory activity (Table S5) further strengthening the hypothesis that VPS34 is the primary target in relation to autophagy inhibition.

To further validate VPS34 as cellular target we treated four different cell lines with azaquindole-1 which resulted in very strong inhibition of LC3 lipidation confirming its autophagy-inhibiting activity (Figures 3h and S7). In addition, ULK1 phosphorylation status in serum starved cells was investigated to confirm that signaling upstream of ULK-1 is not inhibited by azaquindole-1. ULK1 is phosphorylated by mTOR at Ser757 to prevent its interaction with, and activation by, AMPK.[40] Under serum starvation, mTOR is inhibited which reduces ULK1 Ser757 phosphorylation. Dephosphorylated ULK1 interacts with AMPK and promotes VPS34 activation *via* Beclin-1 phosphorylation.[41] Western blot analysis suggests that ULK1 is dephosphorylated in the presence of azaquindole-1, confirming mTOR inhibition (Figures 3i and S7). VPS34 activity *in cellulo* was monitored by WIPI2b puncta formation. WIPI2b is recruited to the autophagosome initiation site in a

PI3P-dependent fashion.[42]. Hek293A cells stably expressing EGFP-WIPI2b[43] were treated with EBSS to induce autophagy in the presence or absence of azaquindole-1 and imaged every 15 seconds for 1 hour. Quantification of the number of WIPI2b foci that appeared over the 1 hour time period showed that azaquindole-1 strongly inhibited WIPI2b puncta formation, similar to wortmannin, and consistent with VPS34 inhibition (Figure 3j-k and Supporting Movies).

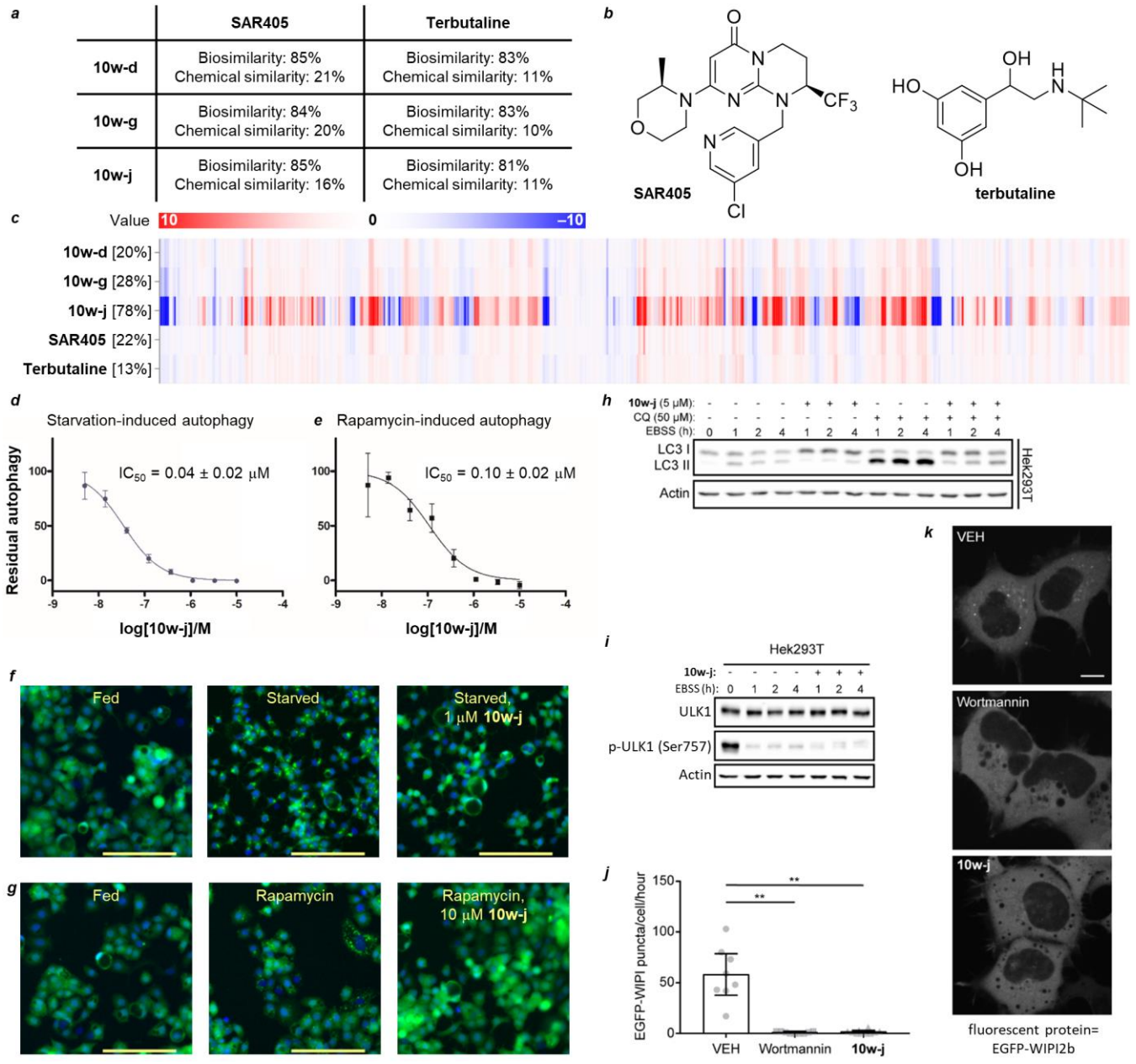

Figure 3. Biological evaluation of the lead compound **10w-j**. (a) Bio- and chemical similarities between selected **10w** compounds and their common reference compounds,[9]); biosimilarity refers to the bioactivity similarity of the cell painting assay "fingerprint" profiles. Chemical similarity refers to the structural similarity of compounds (Tanimoto coefficient);[9] (b) Chemical structures of the reference compounds. (c) Cell painting assay fingerprint profiles for selected **10w** compounds and their biosimilar reference compounds. The percentages in square parenthesis refer to the induction, the fraction of parameters (in %) that underwent significant changes (median absolute deviation [MAD] value) upon compound treatment of at least +/− three-fold of the median determined for the DMSO controls (see also SI Section 5.3);[9] (d) Dose-dependent inhibition of EGFP-LC3 accumulation in MCF7 cells induced by amino acid starvation by Azaquindole-1 (**10w-j**); (e) Dose-dependent inhibition of rapamycin-induced EGFP-LC3 accumulation in MCF7 cells by Azaquindole-1 (**10w-j**); (f) Fluorescence microscopy images of the starvation-induced autophagy screen; (g) Fluorescence

microscopy images of the rapamycin-induced autophagy screen. Blue= Hoechst; green= EGFP-LC3. Scale bars: 150 μm. Data are given as the mean ± SD, *n* ≥ 3, representative graphs and images shown; (h) Western blot analysis of LC3 lipidation in Hek293T cells undergoing starvation in the presence or absence of **10w-j** or chloroquine (CQ), as indicated; (i) Western blot analysis of ULK1 phosphorylation status in starved Hek293T cells when treated with **10w-j**; (j) Quantification of the total number of EGFP-WIPI2b foci appearing during 1 h of EBSS treatment with or without **10w-j** in Hek293A cells stably expressing EGFP-WIPI2b. Bars show mean ± SD from four biologically independent experiments. Data points represent individual cells pooled from independent experiments. Significance was determined from biological replicates using a two-tailed, unpaired t-test. **P≤0.01; (k) Representative fluorescence images of Hek293A EGFP-WIPI cells after 1 h of treatment from ***h***. Scale bars, 10 μm. See Figures S6-7 for versions of western blots ***f-g*** using alternative cell lines.

In-cell target engagement of VPS34 was demonstrated by means of a cellular thermal shift assay (CETSA).[44] An average stabilisation of 5.03 ± 1.8 °C was observed in cell lysate (Figure 4a-b). To determine the mode of VPS34 inhibition we investigated the kinetics for inhibition of VPS34 by azaquindole-1 (**10w-j**), which indicated that it was an ATP competitive inhibitor (Figure 4c).

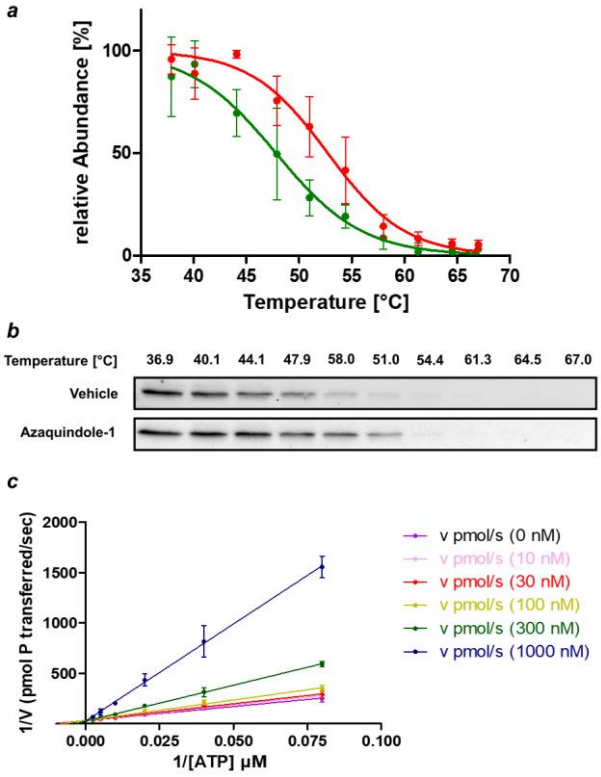

Figure 4. (a) Cellular Thermal Shift Assay (CETSA) for the binding of azaquindole-1 (**10w-j**) to VPS34 in cell lysate (green line = VEH; red line = **10w-j**). Data is mean ± SD, *n* = 3; (b) Representative CETSA blot. See SI Section 5.8 for further details; (c) Lineweaver–Burk plot for inhibition of VPS34 by **10w-j**. Data is mean ± SD, *n* = 3.

We compared the cell painting profile of azaquindole-1 against other recently identified autophagy inhibitors[11,29,38,39,45,46] (Figures S10-11). Our analysis revealed that azaquindole-1 (**10w-j**) was biosimilar to oxautin-1, autoquin and autophinib. Notably, autophinib is a known VPS34 inhibitor, and the cell painting

analysis further validates this earlier finding. The ability of the cell painting assay data to suggest and subsequently identify molecular targets is therefore apparent. However, oxautin-1 and autoquin do not inhibit VPS34. This suggests that the profile may represent compound bioactivity in a broader sense. Thus, the cell painting assay may be a good experimental means to identify clusters of compounds that exhibit similar phenotypic outputs, but not necessarily through the same modes of action. These insights will be investigated more thoroughly in a forthcoming study.

In conclusion, we have reported a novel approach to prepare a new class of pseudo-natural product autophagy inhibitors by fusing the indole ring-system with the cinchona alkaloid scaffold in a biologically unprecedented manner. The lead compound azaquindole-1 (**10w-j**) appears to suppress autophagy by inhibiting the lipid kinase VPS34, as identified by phenotypic profiling using the cell painting assay. These results highlight the potential of the cell painting assay as a target identification technique. Our synthetic strategy may now be extended to investigate alternative modes of indole fusion, and to harness alternative alkaloids (and other natural products) to make numerous new classes of pseudo-natural products that are not available to nature through biosynthesis, and which may be endowed with unique biological activities.

Acknowledgements

D.J.F. thanks the European Commission for a Marie Skłodowska-Curie European Fellowship (Grant 794259). D.P.C. thanks the Canadian Institute of Health Research for a fellowship (MFE-152550). L.L. thanks the Alexander von Humboldt Foundation for funding. We thank Dr Sharon Tooze for providing the Hek293A EGFP-WIPI2b cells. We acknowledge the Biochemical Imaging Center (BICU) at Umeå University and the National Microscopy Infrastructure, NMI (VR-RFI 2016-00968) for assistance with microscopy. We thank Oliver Bartels for routine chemical synthesis. This work was supported by the Max Planck Society (to H.W.), and by ERC (ChemBioAP), Vetenskapsrådet (Nr. 2018-04585), and the Knut and Alice Wallenberg Foundation (to Y-W.W.).

References

[1] D. J. Newman, G. M. Cragg, *J. Nat. Prod.* **2016**, *79*, 629–661.

[2] C. R. Pye, M. J. Bertin, R. S. Lokey, W. H. Gerwick, R. G. Linington, *Proc. Natl. Acad. Sci. U. S. A.*

2017, *114*, 5601–5606.

[3] S. Wetzel, R. S. Bon, K. Kumar, H. Waldmann, *Angew. Chem. Int. Ed.* **2011**, *50*, 10800–10826.

[4] K. C. Morrison, P. J. Hergenrother, *Nat. Prod. Rep.* **2014**, *31*, 6–14.

[5] D. J. Foley, P. G. E. Craven, P. M. Collins, R. G. Doveston, A. Aimon, R. Talon, I. Churcher, F. von Delft, S. P. Marsden, A. Nelson, *Chem. Eur. J.* **2017**, *23*, 15227–15232.

[6] G. Karageorgis, E. S. Reckzeh, J. Ceballos, M. Schwalfenberg, S. Sievers, C. Ostermann, A. Pahl, S. Ziegler, H. Waldmann, *Nat. Chem.* **2018**, *10*, 1103–1111.

[7] T. Schneidewind, S. Kapoor, G. Garivet, G. Karageorgis, R. Narayan, G. Vendrell-Navarro, A. P. Antonchick, S. Ziegler, H. Waldmann, *Cell Chem. Biol.* **2019**, *26*, 512-523.e5.

[8] G. Karageorgis, D. J. Foley, L. Laraia, H. Waldmann, *Nat. Chem.* **2020**, accepted.

[9] A. Christoforow, J. Wilke, A. Binici, A. Pahl, C. Ostermann, S. Sievers, H. Waldmann, *Angew. Chem. Int. Ed.* **2019**, *58*, 14715–14723.

[10] J. Ceballos, M. Schwalfenberg, G. Karageorgis, E. S. Reckzeh, S. Sievers, C. Ostermann, A. Pahl, M. Sellstedt, J. Nowacki, M. A. Carnero Corrales, et al., *Angew. Chem. Int. Ed.* **2019**, DOI 10.1002/anie.201909518.

[11] H. Waldmann, L. Laraia, G. Garivet, D. J. Foley, N. Kaiser, S. Müller, S. Zinken, T. Pinkert, J. Wilke, D. Corkery, et al., *Angew. Chem. Int. Ed.* **2019**, DOI 10.1002/anie.201913712.

[12] B. Over, S. Wetzel, C. Grütter, Y. Nakai, S. Renner, D. Rauh, H. Waldmann, *Nat. Chem.* **2013**, *5*, 21–28.

[13] S. E. O'Connor, J. J. Maresh, *Nat. Prod. Rep.* **2006**, *23*, 532–547.

[14] K. M. Kacprzak, in *Natural Products*, Springer Berlin Heidelberg, Berlin, Heidelberg, **2013**, pp. 605–641.

[15] C. Chen, D. R. Lieberman, R. D. Larsen, T. R. Verhoeven, P. J. Reider, *J. Org. Chem.* **1997**, *62*, 2676–2677.

[16] F. I. Carroll, P. Abraham, K. Gaetano, S. W. Mascarella, R. A. Wohl, J. Lind, K. Petzoldt, *J. Chem. Soc. Perkin Trans. 1* **1991**, 3017–3026.

[17] D. E. Portlock, D. Naskar, L. West, W. L. Seibel, T. Gu, H. J. Krauss, X. S. Peng, P. M. Dybas, E. G. Soyke, S. B. Ashton, et al., *Tetrahedron Lett.* **2003**, *44*, 5365–5368.

[18] P. Ertl, S. Roggo, A. Schuffenhauer, *J. Chem. Inf. Model.* **2008**, *48*, 68–74.

[19] A. P. Bento, A. Gaulton, A. Hersey, L. J. Bellis, J. Chambers, M. Davies, F. A. Krüger, Y. Light, L. Mak, S. McGlinchey, et al., *Nucleic Acids Res.* **2014**, *42*, D1083–D1090.

[20] D. S. Wishart, Y. D. Feunang, A. C. Guo, E. J. Lo, A. Marcu, J. R. Grant, T. Sajed, D. Johnson, C. Li, Z. Sayeeda, et al., *Nucleic Acids Res.* **2018**, *46*, D1074–D1082.

[21] I. Colomer, C. J. Empson, P. Craven, Z. Owen, R. G. Doveston, I. Churcher, S. P. Marsden, A. Nelson, *Chem. Commun.* **2016**, *52*, 7209–7212.

[22] F. Lovering, J. Bikker, C. Humblet, *J. Med. Chem.* **2009**, *52*, 6752–6756.

[23] D. J. Foley, A. Nelson, S. P. Marsden, *Angew. Chem. Int. Ed.* **2016**, *55*, 13650–13657.

[24] C. A. Lipinski, F. Lombardo, B. W. Dominy, P. J. Feeney, *Adv. Drug Deliv. Rev.* **1997**, *23*, 3–25.

[25] RDKit: Open-Source Cheminformatics Software. http://rdkit.org. Last visited 28/05/2018.

[26] Y. Wang, A. Cornett, F. J. King, Y. Mao, F. Nigsch, C. G. Paris, G. McAllister, J. L. Jenkins, *Cell Chem. Biol.* **2016**, *23*, 862–874.

[27] B. K. Wagner, S. L. Schreiber, *Cell Chem. Biol.* **2016**, *23*, 3–9.

[28] A. Friese, A. Ursu, A. Hochheimer, H. R. Schöler, H. Waldmann, J. M. Bruder, *Cell Chem. Biol.* **2019**, *26*, 1050–1066.

[29] L. Laraia, K. Ohsawa, G. Konstantinidis, L. Robke, Y. W. Wu, K. Kumar, H. Waldmann, *Angew. Chem. Int. Ed.* **2017**, *56*, 2145–2150.

[30] D. C. Rubinsztein, P. Codogno, B. Levine, *Nat. Rev. Drug Discov.* **2012**, *11*, 709–730.

[31] S. He, Q. Li, X. Jiang, X. Lu, F. Feng, W. Qu, Y. Chen, H. Sun, *J. Med. Chem.* **2018**, *61*, 4656–4687.

[32] G. Konstantinidis, S. Sievers, Y.-W. Wu, Humana Press, New York, NY, **2018**, pp. 187–195.

[33] S. M. Gustafsdottir, V. Ljosa, K. L. Sokolnicki, J. A. Wilson, D. Walpita, M. M. Kemp, K. P. Seiler, H. A. Carrel, T. R. Golu, S. L. Schreiber, et al., *PLoS One* **2013**, *8*, e80999.

[34] M. A. Bray, S. Singh, H. Han, C. T. Davis, B. Borgeson, C. Hartland, M. Kost-Alimova, S. M. Gustafsdottir, C. C. Gibson, A. E. Carpenter, *Nat. Protoc.* **2016**, *11*, 1757–1774.

[35] J. C. Caicedo, S. Cooper, F. Heigwer, S. Warchal, P. Qiu, C. Molnar, A. S. Vasilevich, J. D. Barry, H. S. Bansal, O. Kraus, et al., *Nat. Methods* **2017**, *14*, 849–863.

[36] B. Melillo, J. Zoller, B. K. Hua, O. Verho, J. C. Borghs, S. D. Nelson, M. Maetani, M. J. Wawer, P. A.

Clemons, S. L. Schreiber, *J. Am. Chem. Soc.* **2018**, *140*, 11784–11790.

[37] M. J. Wawer, K. Li, S. M. Gustafsdottir, V. Ljosa, N. E. Bodycombe, M. A. Marton, K. L. Sokolnicki, M.-A. Bray, M. M. Kemp, E. Winchester, et al., *Proc. Natl. Acad. Sci. U. S. A.* **2014**, *111*, 10911–6.

[38] L. Robke, L. Laraia, M. A. Carnero Corrales, G. Konstantinidis, M. Muroi, A. Richters, M. Winzker, T. Engbring, S. Tomassi, N. Watanabe, et al., *Angew. Chem. Int. Ed.* **2017**, *56*, 8153–8157.

[39] L. Robke, Y. Futamura, G. Konstantinidis, J. Wilke, H. Aono, Z. Mahmoud, N. Watanabe, Y.-W. Wu, H. Osada, L. Laraia, et al., *Chem. Sci.* **2018**, *9*, 3014–3022.

[40] J. Kim, M. Kundu, B. Viollet, K. L. Guan, *Nat. Cell Biol.* **2011**, *13*, 132–141.

[41] R. C. Russell, Y. Tian, H. Yuan, H. W. Park, Y.-Y. Chang, J. Kim, H. Kim, T. P. Neufeld, A. Dillin, K.-L. Guan, *Nat. Cell Biol.* **2013**, *15*, 741–750.

[42] H. E. J. Polson, J. de Lartigue, D. J. Rigden, M. Reedijk, S. Urbé, M. J. Clague, S. A. Tooze, *Autophagy* **2010**, *6*, 506–522.

[43] H. C. Dooley, M. Razi, H. E. J. Polson, S. E. Girardin, M. I. Wilson, S. A. Tooze, *Mol. Cell* **2014**, *55*, 238–252.

[44] D. Martinez Molina, P. Nordlund, *Annu. Rev. Pharmacol. Toxicol.* **2016**, *56*, 141–161.

[45] L. Robke, T. Rodrigues, P. Schröder, D. J. Foley, G. J. L. Bernardes, L. Laraia, H. Waldmann, *Tetrahedron* **2018**, *74*, DOI 10.1016/j.tet.2018.07.021.

[46] L. Laraia, A. Friese, D. P. Corkery, G. Konstantinidis, N. Erwin, W. Hofer, H. Karatas, L. Klewer, A. Brockmeyer, M. Metz, et al., *Nat. Chem. Biol.* **2019**, *15*, 710–720.

10.1002/anie.202000364

Table of contents graphic: